

doi:10.15199/48.2017.08.40

A two-phase sine wave generator dedicated for impedance comparison systems

Abstract. The hardware idea and experimental studies of a two-phase sine wave generator intended for use in an impedance metrology are described. The scope of the study involved determining the parameters of the generator that significantly affect its applicability in precise impedance measurements, i.e.: amplitude and phase stability of generated sinewave signals, as well as the total harmonic distortion and the spurious-free dynamic range, which determine their dynamic properties.

Streszczenie. W artykule przedstawiono rozwiązanie układowe oraz wyniki badań eksperymentalnych dwufazowego generatora sygnałów sinusoidalnych przeznaczonego do stosowania w metrologii impedancyjnej. Zakres badań obejmował wyznaczenie parametrów generatora, które w istotny sposób wpływają na jego możliwości aplikacyjne w układach do precyzyjnego porównywania impedancji, t.j.: stabilność amplitudy i fazy generowanych sygnałów sinusoidalnych oraz współczynnik zawartości harmonicznych i zakres dynamiczny bez zniekształceń, określające ich właściwości dynamiczne. (Dwufazowy generator sygnałów sinusoidalnych przeznaczony do zastosowania w układach do porównań impedancji).

Keywords: two-phase generator, impedance measurement, complex voltage ratio.

Słowa kluczowe: generator dwufazowy, pomiary impedancji, zespolony stosunek napięć.

Introduction

Digital multi-phase sine wave voltage generators play an important role in precise impedance measurements, especially in impedance bridges where they are used for various purposes and determine the measurement accuracy [1-3]. One of the uses of two-phase generators is reproduction of the complex voltage ratio ensuring the main balance of a digital impedance bridge [4-9]. In some digitally assisted bridges [10-15] as well as full digital bridges [16-18], digital multiphase generators are used to compensate voltages in selected nodes of the bridge to fulfil four terminal-pair definition of impedances under comparison.

Such generators for impedance metrology purposes are based on top class digital-to-analog converters (DACs). In addition to the high resolution of these DACs and their excellent dynamic parameters, dc parameters are also important – especially a gain and offset temperature coefficient. For this reason, sigma-delta DACs are used less often than R-2R DACs, despite of their excellent dynamic parameters.

This paper describes an improved version of a digital two-phase sine wave voltage generator presented in [19] and build on the 20-bit R-2R Analog Devices AD5791 DACs. Details of the improvement are described in the next section. The applied DAC stands out, from other commercial DACs with the resolution equal or greater than 20-bit, due to its excellent ac and dc parameters.

Experimental studies of the generator parameters, important due to its application in an impedance comparison system, are widely presented too. The parameters presented in [19] concerned only the 1-kHz signal. Now, the frequency range of studies has been extended to the whole acoustic frequency band. Besides the stability of the amplitude ratio and the phase shift between the generated signals, a spectral purity of the signals is also presented.

Design of the generator

The block diagram of the designed generator is presented in Fig. 1. It consists of three functional blocks. The first one creates synchronously and sequentially discrete-time, discrete-valued representation of the sine waveform and is commonly called a numerically controlled oscillator (NCO). The second block contains DACs creating, in combination with NCO, a direct digital synthesizer (DDS). To obtain at the DAC output a pure sine wave, a low-pass reconstruction filter was applied, which is the third block of the generator.

In the described generator NCO has been implemented in software running on an ARM Cortex-M7 series microcontroller. It calculates the discrete values of sinusoidal signal samples for both channels, converts them into appropriate codes and sends them to DACs. Comparing to the previous version [19], NCO has been

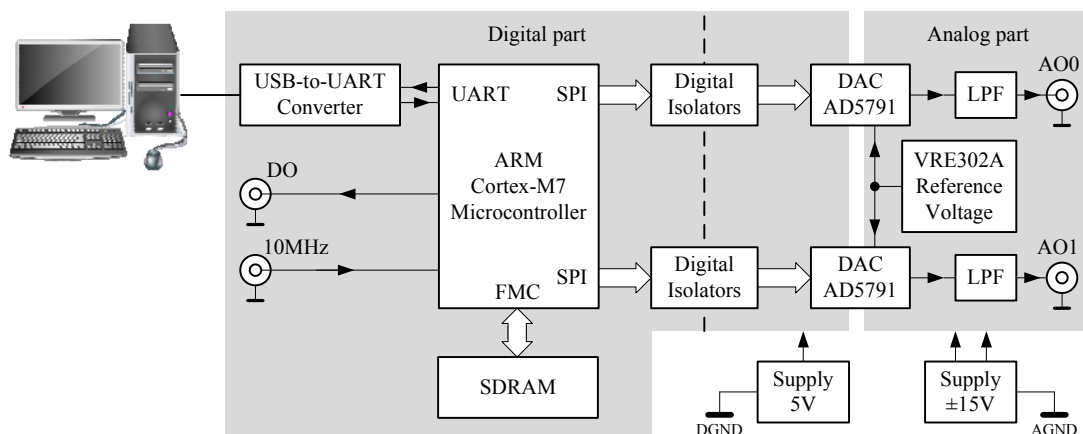


Fig. 1. Block diagram of the two-phase sine wave generator.

simplified. Instead of two microcontrollers only one has been used. Such an approach not only simplifies the NCO design but in particular facilitates the synchronous transmission of samples to DACs.

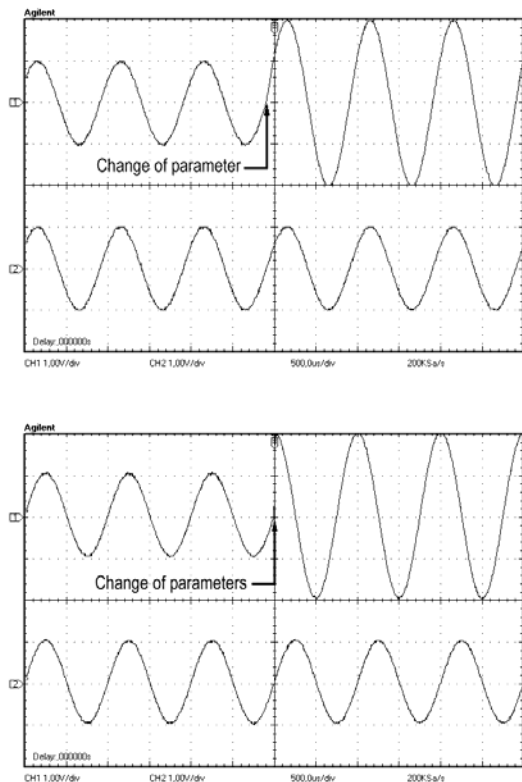


Fig.2. The moment of the amplitude change from 1 V to 2 V in one channel (top oscilloscope screenshot) and the simultaneous change of the amplitude from 1 V to 2 V and the phase from 0° to 90° (bottom oscilloscope screenshot).

The remaining part of generator was unchanged. Therefore, as the reference voltage, common for both channels of the generator, the VRE302A chip is used. Also, to remove images, appearing around each integer multiple of the DAC update rate, a 40-kHz low-pass third-order Butterworth filter (LPF) is connected to each DAC output.

The simultaneous changes of the voltage at the outputs of both DACs during the generation of the sine wave are achieved by linking the timing of the DAC code uploading to the reference clock signal. The reference clock signal can be determined on the basis of the internal clock timing of the microcontroller or on an external reference 10-MHz signal. Each falling edge of the 500-kHz reference clock starts the procedure of sending a new code through the SPI interface to DACs and the rising edge updates the voltages at the DACs output.

To enable a synchronization of the generator with other devices, such as a lock-in amplifier, a logic signal of the same frequency as the frequency of the signals at AO0 and AO1 analog outputs is generated at DO output.

The generator is controlled from a personal computer (PC), which runs program for setting the amplitude, phase and frequency of the generated signals. The connection between PC and the generator is made via an USB interface.

The microcontroller firmware uses three buffers to store all samples of both waveforms. Two buffers store samples of the currently generated signals. The third one is used to store the samples of a new required waveform. When data of the new waveform are prepared, pointers to the buffers

are swapped. Then, the released buffer can be used for storing new samples for next change of the amplitude or phase. An exchange of the pointers is a very fast process, so both the amplitude and phase can be changed during the signal generation (Fig. 2). The frequency of signals can be changed only when the generation is stopped.

Evaluation of the generator properties

There are several criteria to evaluate the quality of the generated signals. Stability of the amplitude ratio and phase shift between the generated signals are two of most important properties of two-phase generators for impedance ratio measurement applications. In the particular case, when impedances characterized by the module of a similar nominal value are compared, and the interchange procedure is applied, the comparison result depends mainly on the relative stability of the generated voltages [17].

The noise-related parameters like the total harmonic distortion (THD) and the spurious-free dynamic range (SFDR) are also examined. Their importance results from the fact that in the impedance comparison system a null detector has to measure a complex voltage at the level of several microvolts. High THD or low SFDR makes impossible to reach the balance condition with suitable accuracy.

Stability of Amplitude Ratio and Phase Shift

The stability of the amplitude ratio and the phase shift was carried out in the measurement setup based on the 24-bit digitizer PXI-4461 working in a sequential mode, where two measured signals are sampled by a single input channel of the digitizer [20]. The sequential switching of the generated signals was carried out by an in house made two channel multiplexer.

To achieve a coherent sampling, the sampling frequency in the digitizer was synchronized with the same 10-MHz clock signal which was used to derive the update rate in the tested generator. The switching frequency of the multiplexer was also synchronized with 10-MHz clock signal.

Every 0.08 s the digitizer took sequentially 4096 samples of each of the two signals with the sampling rate of 102.4 kHz. Only 2048 samples within the middle of each sequence were taken to calculate the discrete Fourier transform and then the amplitude ratio and phase shift.

Overall time for measurements at each frequency was about four hours. Due to the linear change of the temperature in the laboratory during the measurement, further calculations were corrected for influence of temperature on measurements. Temperature coefficients of the amplitude ratio and phase shift are about 1.5 ppm/°C and -0.3 μ rad/°C, respectively.

Noise influence on measurements was removed by means of averaging. Figs. 3 and 4 show the stability of the amplitude ratio and phase shift for two values of the averaging window length (10 s and 100 s, respectively). The same range of the Y axis on Figs. 3 and 4 shows that a tenfold increase in the averaging time results in more than two fold improvement of the amplitude ratio and phase shift stability. Table I shows the results obtained for the two other signal frequencies too.

The measurements devoid of the linear drift are also used to compute the overlapping Allan deviation. Fig. 5 presents the Allan deviation plots for two signal frequencies. As can be seen, for averaging time shorter than 100 s (resp. for phase shift of the 10-kHz signal is about 20 s), the Allan deviation decreases with the slope of -0.5. It means that the noise is mainly white and the averaging can be used for reduction of dispersion of the measurements. For

the 1 kHz signal and the averaging time above 100 s, the 1/f noise limits the accuracy of the phase shift measurements. In case of the 10-kHz signal, increasing the averaging time from 20 s to 100 s does not significantly reduce the noise on the measurements of the phase shift. Conclusions made from Allan deviation measurements are

in agreement with data presented in Table 1, which show that the dispersion of the phase shift was improved about two times for 10 kHz compared to the three-time improvement for the 1-kHz signal.

Table 1. Dispersion of the amplitude ratio and phase shift measured over four hours

Avg. time (s) →	10	100	10	100
Signal frequency (Hz) ↓	Amplitude ratio (μV/V)		Phase shift (μrad)	
100	0.79	0.24	0.57	0.17
1000	0.62	0.25	0.43	0.14
10000	1.13	0.25	2.58	1.26

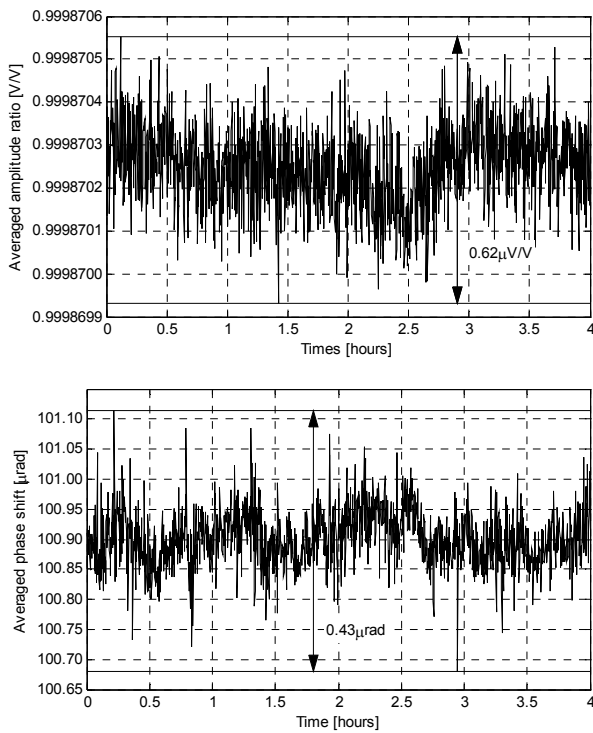


Fig.3. Stability of the amplitude ratio (top) and phase shift (bottom) of the 5-V amplitude signals measured at frequency of 1 kHz. Applied averaging window is 10 s.

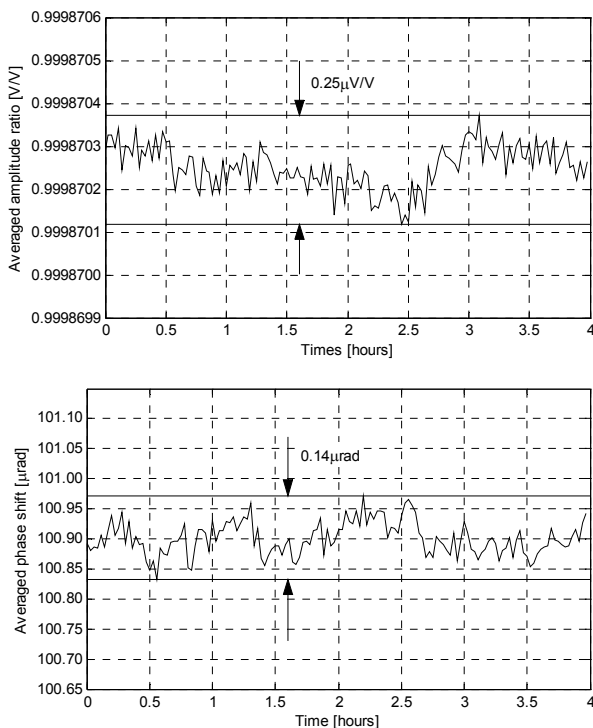


Fig.4. Stability of the amplitude ratio (top) and phase shift (bottom) of the 5-V amplitude signals measured at frequency of 1 kHz. Applied averaging window is 100 s.

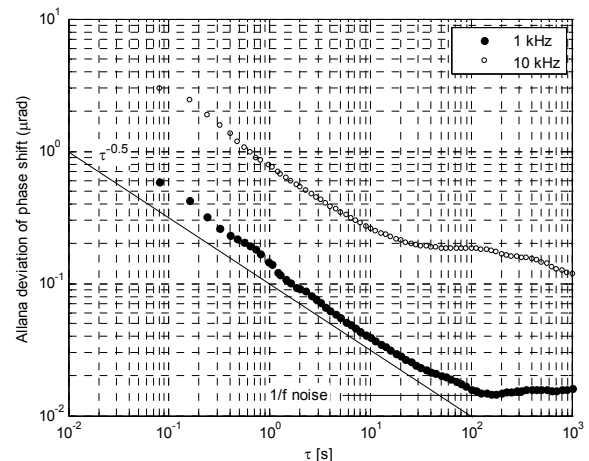
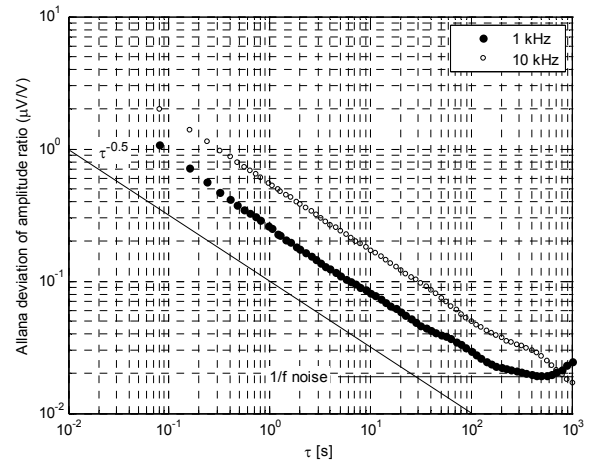


Fig.5. Overlapping Allan deviation of the amplitude ratio (top) and phase shift (bottom) measured at the 1-kHz and 10-kHz signals. The solid lines are only for guide.

Spectral purity of the generated signals

The measurements of THD and SFDR were performed for two amplitudes: 1 V and 5 V, and the frequencies of generated signals from 20 Hz to 20 kHz by the PXI 5922 digitizer with sampling frequency of 1 MHz, which ensured 22-bit resolution of the digitizer. For the amplitude of 1 V, which corresponds to the one fifth of the full voltage range, THD increases from about 0.01% at 20 Hz up to 0.03% at 20 kHz. When the amplitude increases to the full voltage range, the signals generated at the frequencies up to 2 kHz are characterized by THD not higher than about 0.0046%. For the frequency of 10 kHz and above THD increases up to 0.16% (for 20 kHz). Reasons for increasing THD are dynamic properties of DAC, which cause imperfections in steps used to generate the waveform. With the increase of the output signal frequency, when the signal is generated

from a small number of samples per period, and which corresponds to high changes of the voltage at the output of DAC, the decisive influence on the shape of steps has the slow rate of the DAC output operational amplifier.

SFDRs for frequencies covering the whole frequency range of the generator are presented in Table 2. For frequencies up to 5 kHz better performance is obtained when the amplitude is closer to the full voltage range. For higher frequencies the dynamic properties of the output stage of DAC cause that the higher SFDR is obtained for the 1-V amplitude signal when the amplitude of steps is small.

Table 2. The spurious-free dynamic range measured in dBc for each channel for different frequencies of generated signals and two amplitudes.

Frequency (Hz)	Amplitude 1 V		Amplitude 5 V	
	AO0	AO1	AO0	AO1
20	86.3	86.1	99.7	98.9
100	82.1	82.1	96.1	95.1
200	82.8	83.1	97.2	96.3
500	82.6	82.4	94.3	95.0
1000	82.5	82.5	91.6	92.7
2000	81.3	81.5	89.9	90.9
5000	76.7	77.0	79.1	80.4
10000	75.4	75.0	59.9	61.0
20000	70.7	70.5	57.1	57.9

Conclusions

In the paper the experimental study of the relative stability and the dynamic parameters of the two-phase sine wave generator based on the commercially available 20-bit DACs are described. The generated signals of the full-scale amplitude in the band of 20 Hz to 2 kHz are characterized by THD not higher than 0.0046% and SFDR not lower than 90 dBc. The studies of the stability shown, that for the signal of 1 kHz and averaging time of 100 s the generator is able to maintain the stability of the amplitude ratio and phase shift on the level of $\pm 0.13 \mu\text{V/V}$ and $\pm 0.07 \mu\text{rad}$, respectively, within the time of four hours. The very good performance, especially for frequencies up to 1 kHz, makes it possible to use this generator in impedance comparison systems.

This work was partially carried out with funding by the European Union within the EMRP Joint Research Project AIM QuTE. The EMRP is jointly funded by the EMRP participating countries within EURAMET and the European Union.

Authors: Miroslaw Koziol, Ph.D., Janusz Kaczmarek, Ph.D., Ryszard Rybski, Ph.D., D.Sc., University of Zielona Góra, Institute of Metrology, Electronics and Computer Science, ul. Prof. Z. Szafrana 2, 65-516 Zielona Góra, Poland, E-mail: m.koziol@imei.uz.zgora.pl, j.kaczmarek@imei.uz.zgora.pl, r.rybski@imei.uz.zgora.pl; Jan Kučera, Ph.D., Czech Metrology Institute, Okružní 31, CZ-638 00 Brno, Czech Republic, E-mail: jkučera@cmi.cz.

REFERENCES

- [1] Ramm G., Impedance Measuring Device Based on an AC Potentiometer, *IEEE Trans. Instrum. Meas.*, 34 (1985), No. 2, 341-344
- [2] Callegaro L., Galzerano G., Svelto C., A multiphase direct-digital-synthesis sinewave generator for high-accuracy impedance comparison, *IEEE Trans. Instrum. Meas.*, 50 (2001), No. 4, 926-929
- [3] Overney F., Jeanneret B., Realization of an inductance scale traceable to the quantum Hall effect using an automated synchronous sampling system, *Metrologia*, 47 (2010), No. 6, 690-698
- [4] Bachmair H., Vollmert R., Comparison of Admittances by Means of a Digital Double-Sinewave Generator, *IEEE Trans. Instrum. Meas.*, 29 (1980), No. 4, 370-372
- [5] Helbach W., Marcinowski P., Trenkler G., High-Precision Automatic Digital AC Bridge, *IEEE Trans. Instrum. Meas.*, 32 (1983), No. 1, 159-162
- [6] Waltrip B.C., Oldham N.M., Digital impedance bridge, *IEEE Trans. Instrum. Meas.*, 44 (1995), No. 2, 436-439
- [7] Ramm G., Moser H., From the calculable AC resistor to capacitor dissipation factor determination on the basis of the time constants, *IEEE Trans. Instrum. Meas.*, 50 (2001), No. 2, 286-289
- [8] Rybski R., Impedance comparison in a circuit with two digital sinewave generators", *Metrology and Measurement Systems*, 11 (2004), No. 2, 131-145
- [9] Ramm G., Moser H., New multifrequency method for the determination of the dissipation of capacitors and of the time constant of resistors, *IEEE Trans. Instrum. Meas.*, 54 (2005), No. 2, 521-524
- [10] Muciek A., Digital impedance bridge based on a two-phase generator, *IEEE Trans. Instrum. Meas.*, 46 (1997), No. 2, 467-470
- [11] Trinchera B., Callegaro L., D'Elia V., Quadrature bridge for R-C comparisons based on polyphase digital synthesis, *IEEE Trans. Instrum. Meas.*, 58 (2009), No. 1, 202-206
- [12] Callegaro L., D'Elia V., Trinchera B., Realization of the farad from the dc quantum Hall effect with digitally assisted impedance bridges, *Metrologia*, 47 (2010), No. 4, 464-472
- [13] Lan J., Zhang Z., Li Z., He Q., Zhao J., Lu Z., A digital compensation bridge for R-C comparisons", *Metrologia*, 49 (2012), No. 3, 266-272
- [14] Trinchera B., D'Elia V., Callegaro L., A Digitally Assisted Current Comparator Bridge for Impedance Scaling at Audio Frequencies, *IEEE Trans. Instrum. Meas.*, 62 (2013), No. 6, 1771-1775
- [15] Callegaro L., D'Elia V., Kučera J., Ortolano M., Pourdanesh F., Trinchera B., Self-Compensating Networks for Four-Terminal-Pair Impedance Definition in Current Comparator Bridges, *IEEE Trans. Instrum. Meas.*, 65 (2016), No. 5, 1149-1155
- [16] Overney F., Jeanneret B., RLC Bridge Based on an Automated Synchronous Sampling System, *IEEE Trans. Instrum. Meas.*, 60 (2011), No. 7, 2393-2398
- [17] Callegaro L., D'Elia V., Kampik M., Kim D.B., Ortolano M., Pourdanesh F., Experiences With a Two-Terminal-Pair Digital Impedance Bridge, *IEEE Trans. Instrum. Meas.*, 64 (2015), No. 6, 1460-1465
- [18] Rybski R., Kaczmarek J., Kontorski K., Impedance Comparison Using Unbalanced Bridge With Digital Sinewave Voltage Sources, *IEEE Trans. Instrum. Meas.*, 64 (2015), No. 12, 3380-3386
- [19] Koziol M., Kaczmarek J., Rybski R., High-performance two-phase sine wave generator for impedance bridges, XXI IMEKO World Congress, Prague, Czech Republic, 30 August – 4 September 2015
- [20] Rybski R., Kaczmarek J., Koziol M., A High-Resolution PXI Digitizer for a Low-Value-Resistor Calibration System, *IEEE Trans. Instrum. Meas.*, 62 (2013), No. 6, 1783-1788